Journal of Biomechanics 201 (2026) 113259

Contents lists available at ScienceDirect

Journal of Biomechanics

journal homepage: www.elsevier.com/locate/jbiomech

Paretic limb biomechanical response to hip exoskeleton limb assistance strategies during walking for individuals post-stroke

Kristen M. Stewart [a], Gregory S. Sawicki [b,c,d], Aaron J. Young [b,c], Richard R. Neptune [a,*]

[a] Walker Department of Mechanical Engineering, The University of Texas at Austin, Austin, TX, USA
[b] George W. Woodruff School of Mechanical Engineering, Georgia Institute of Technology, Atlanta, GA, USA
[c] Institute for Robotics and Intelligent Machines, Georgia Institute of Technology, Atlanta, GA, USA
[d] School of Biological Sciences, Georgia Institute of Technology, Atlanta, GA, USA

ARTICLE INFO

Keywords:
Gait
Biomechanics
Hip exoskeleton
Assistive devices
Hemiparesis

ABSTRACT

Individuals post-stroke with hemiparetic gait often experience impaired mobility, which can be restored using powered exoskeletons. Specifically, hip exoskeletons can deliver positive work to the leg to help initiate leg swing; however, it is unclear which limb assistance strategy (e.g., unilateral or bilateral assistance) best improves walking performance due to the asymmetric characteristics of hemiparetic gait. Therefore, the purpose of this study was to investigate how different hip exoskeleton limb assistance strategies affect lower-limb joint biomechanics during walking for individuals post-stroke. We hypothesized that bilateral assistance would best improve late stance paretic leg orientation and swing initiation, unilateral paretic limb assistance would improve interlimb asymmetries and unilateral nonparetic limb assistance would indirectly improve late stance kinematics. We found bilateral assistance significantly increased paretic hip flexion angle, providing an improvement in leg swing initiation, and improved ankle joint work symmetry, suggesting an improvement in propulsion mechanics. Unilateral paretic limb assistance significantly increased paretic knee flexion during swing, which is a common rehabilitative target to improve stiff-knee gait for individuals post-stroke, and significantly improved joint work symmetry between limbs, which is beneficial for individuals who have increased reliance on the nonparetic limb. Unilateral nonparetic assistance did not improve late stance kinematics. These results provide insight into joint-level responses of individuals post-stroke and can help tailor hip exoskeleton assistance for individuals post-stroke based on rehabilitation targets.

1. Introduction

Individuals post-stroke commonly experience hemiparesis, with over 80% of strokes leading to motor impairment (Langhorne et al., 2011). Post-stroke hemiparesis is characterized by unilateral muscle weakness, resulting in altered gait patterns. Muscle weakness is often manifested in reduced paretic plantarflexor output that leads to decreased propulsion (e.g., Chen et al., 2005; Bowden et al., 2006), paretic limb muscle work during pre-swing (Peterson et al., 2011) and walking speed (e.g., Olney and Richards, 1996). This reduced plantarflexor output necessitates compensatory mechanisms at other joints, such as increased paretic hip work during pre-swing (Peterson et al., 2011) and reduced paretic knee flexion during swing (e.g., Chen et al., 2005; Dean et al., 2020) compared to healthy individuals. Further, the kinematic and kinetic disparities create asymmetric gait patterns, with an increased reliance on the nonparetic limb. Limb asymmetries are present in muscle function (e.g., greater nonparetic relative to paretic limb muscle contributions to propulsion (Hall et al., 2011)), spatiotemporal measures (e.g., step length asymmetry (Balasubramanian et al., 2009)) and kinetic measures (e.g., reduced paretic propulsion and interlimb mechanical power symmetry (e.g., Bowden et al., 2006; Roelker et al., 2019; Farris et al., 2015; Mahon et al., 2015)). These asymmetries highlight the impaired walking performance of individuals post-stroke, which can result in limited mobility during activities of daily living.

Powered exoskeletons have the potential to improve mobility for individuals post-stroke by delivering external work at targeted joints. Ankle exoskeletons often target improved propulsion (e.g., Awad et al., 2017) but depend on leg orientation in late stance to appropriately

* Corresponding author at: Walker Department of Mechanical Engineering, The University of Texas at Austin, 204 E. Dean Keeton Street Stop C2200, Austin, TX 78712-1591, USA.
E-mail address: rneptune@mail.utexas.edu (R.R. Neptune).

https://doi.org/10.1016/j.jbiomech.2026.113259
Accepted 17 March 2026
Available online 21 March 2026

convert the exoskeleton work to forward propulsion (McCain et al., 2019). However, individuals post-stroke often have reduced leg extension in late stance (Peterson et al., 2010), and therefore hip exoskeletons that are independent of leg orientation and provide positive hip flexor work for leg swing initiation may be advantageous. In healthy adults, hip exoskeleton assistance reduced hip and ankle muscle activity (Lenzi et al., 2013) and metabolic cost (e.g., Seo et al., 2016) relative to unassisted walking, suggesting the exoskeleton may have distal effects. In individuals post-stroke, hip exoskeleton assistance has been shown to improve walking speed and spatiotemporal parameters (e.g., Lee et al., 2019; Pan et al., 2023; Livolsi et al., 2025) relative to unassisted walking. Although walking speed is a valuable clinical measure positively correlated with motor recovery post-stroke (Brandstater et al., 1983), it may reflect nonparetic limb compensations rather than paretic limb functional improvements. Therefore, it remains unclear how these individuals alter their lower-limb joint kinematics and kinetics in response to different powered exoskeleton limb assistance strategies.

To improve walking performance, the exoskeleton's control parameters and assistance strategy must be appropriately tuned. Experimental studies have optimized timing and magnitude of the applied torque to reduce metabolic cost in healthy adults (e.g., Galle et al., 2017; Young et al., 2017; Ding et al., 2018; Bryan et al., 2021). However, optimized assistance for healthy adults typically assumes inter-limb symmetry, which may not generalize to clinical populations. Given the notable post-stroke limb asymmetry, it is unclear how different limb assistance strategies (e.g., unilateral versus bilateral assistance) may impact their walking mechanics. Further, it is unclear whether unilateral paretic or nonparetic limb assistance would be more suitable based on the impaired function of the paretic limb and increased reliance on the nonparetic limb.

The purpose of this study was to investigate how different hip exoskeleton limb assistance strategies affect lower-limb joint biomechanics during walking for individuals post-stroke. We hypothesized that 1) bilateral assistance would best improve paretic limb late stance leg orientation and swing initiation, 2) unilateral paretic limb assistance would best improve limb asymmetries, and 3) unilateral nonparetic limb assistance would indirectly improve paretic limb late stance leg orientation.

2. Methods

2.1. Experimental data collection

Experimental data were previously collected from five individuals post-stroke with chronic unilateral hemiparesis (Table 1), with each participant providing their informed consent for the Georgia Institute of Technology Institutional Review Board approved study. For a more detailed description of the methods, see Pan et al. (2023).

Subjects wore a Samsung Gait Enhancing and Motivating System (Samsung Electronics, Suwon, South Korea), which is a lightweight powered bilateral hip exoskeleton with an additional thoracolumbar interface (total mass: 3.3 kg). The device provided sagittal plane bidirectional assistance and incorporated a passive joint to allow free frontal plane movement. A biological-inspired torque controller was implemented on the exoskeleton, where the commanded flexor/extensor torque was the sum of two univariate Gaussian curves with a maximum commanded torque of 6 Nm (Fig. 1; for more details, see Kang et al., 2021).

During a baseline assessment, individuals walked overground without the exoskeleton to determine their self-selected walking speed. During a second session, the individuals donned the exoskeleton, and a clinician tuned the onset assistance timing within ± 5% of the gait cycle to ensure the individuals' comfort and acclimation to the device. During a third session, they walked on a split-belt instrumented treadmill (Bertec, Ohio, USA) at 80% of their self-selected overground walking speed with the exoskeleton. Exoskeleton assistance conditions were randomized across trials and included unassisted (UN), unilateral-paretic limb (P), unilateral-nonparetic limb (NP) and bilateral (BI) assistance conditions. Three-dimensional motion capture data were collected from thirty-five lower-limb retroreflective markers at 200 Hz (Vicon Motion Systems, Oxford, United Kingdom) and ground reaction force data were collected from the treadmill at 1000 Hz.

2.2. Data analysis

Kinematic and kinetic data were filtered with a 4th order low-pass Butterworth filter at 6 Hz and 15 Hz, respectively. For each subject, an eight-segment inverse dynamics model was created in Visual3D (HAS-Motion, Ontario, Canada), and paretic and nonparetic sagittal plane hip, knee and ankle joint angles, and net joint moments and powers were calculated for each trial. Net joint moments and powers include both the biological and exoskeleton dynamics. All data were divided into gait cycles and normalized to 100% of the gait cycle. Peak kinematic and kinetic values and total joint range of motion (ROM) were identified over the gait cycle. Positive, negative and total joint moment impulse and work were calculated as the time integral of joint moments and powers, respectively, over each gait cycle. To evaluate work symmetry, joint work distribution was quantified as the proportion of each joint's positive or negative work relative to the total positive or negative work, respectively, across both lower limbs. Joint moments, powers and work were normalized by subject mass.

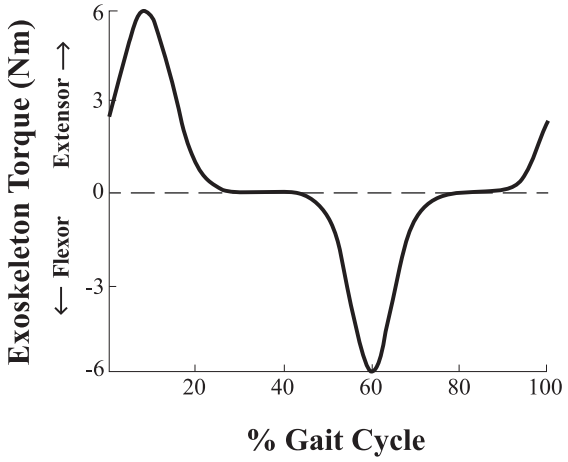

Fig. 1. Exoskeleton torque commanded for the ipsilateral leg.

Table 1
Subject demographics and characteristics.

Subject	Sex	Age	Height (cm)	Mass (kg)	Paretic Side	Time Post-Stroke (years)	Self-Selected Walking Speed (m/s)	Prescribed Assistive Device?
1	M	37	180.5	89.0	Right	6	0.64	Yes
2	M	57	175.5	81.0	Left	9	0.86	Yes
3	M	55	183.0	84.8	Right	3	0.60	Yes
4	F	67	156.0	57.9	Left	3	0.98	No
5	F	46	167.5	59.9	Right	4	1.00	No

2.3. Statistical analysis

Linear mixed effects models were used to evaluate differences in outcome measures between limb assistance conditions. Separate models were created to analyze outcome measures of joint ROM, peak joint angle, moment and power, joint moment impulse and positive, negative and total work for the hip, knee and ankle of the paretic limb. The model included a categorical fixed effect of limb assistance condition (i.e., UN, P, NP or BI) and a random intercept of subject to account for baseline functional differences between individuals. If a significant effect of assistance strategy was found, follow-up paired t-tests with a Bonferroni correction were performed between the UN condition and each powered condition. The normality assumption was assessed by visual inspection of the residual Q-Q plot for each model, which did not indicate substantial deviations from normality. Significance was set as $\alpha = 0.05$. All statistical analyses were performed in the MATLAB statistical toolbox (MathWorks, Massachusetts, USA).

3. Results

3.1. Paretic limb kinematics

Peak paretic limb hip flexion angle increased in all powered conditions (P: $p = 0.004$; NP: $p < 0.001$; BI: $p < 0.001$) (Fig. 2A) relative to UN. However, peak hip extension angle decreased only in the P condition ($p = 0.002$) (Fig. 2A) relative to UN. Hip ROM increased in the NP ($p = 0.003$) and BI ($p = 0.001$) conditions relative to UN.

Peak paretic limb knee flexion increased only in the P condition ($p = 0.002$) and knee ROM increased only in the P condition ($p < 0.001$) relative to UN (Fig. 2B).

There were no changes in paretic limb ankle kinematics with any assistance condition relative to UN (Fig. 2C). The average peak and ROM magnitudes for each joint are provided in Appendix A1 and additional linear mixed effects model details are provided in Appendix B1.

3.2. Paretic limb net joint moments

Peak paretic limb hip extensor moments increased in all powered conditions (P: $p < 0.001$; NP: $p < 0.001$; BI: $p = 0.003$) and peak hip flexor moments decreased in all powered conditions (P: $p = 0.041$; NP: $p = 0.008$; BI: $p = 0.017$) relative to UN (Fig. 3A). Similarly, hip extensor moment impulse increased in all powered conditions (P: $p = 0.010$; NP: $p = 0.006$; BI: $p = 0.002$) and hip flexor moment impulse decreased in all powered conditions (P: $p < 0.001$; NP: $p = 0.001$; BI: $p = 0.001$) relative to UN.

Peak paretic limb knee flexor moment increased in the BI condition ($p = 0.026$) and knee extensor moment impulse decreased in the P ($p = 0.016$) and NP ($p = 0.050$) conditions relative to UN (Fig. 3B).

Peak paretic limb plantarflexor moment increased in the P condition ($p < 0.001$), and peak dorsiflexor moment decreased in the NP condition ($p = 0.041$) relative to UN (Fig. 3C). Ankle dorsiflexor moment impulse decreased in all powered conditions (P: $p = 0.010$; NP: $p = 0.002$; BI: $p = 0.033$) relative to UN. The average peak joint moment and impulses for each joint are provided in Appendix A2 and additional linear mixed effects model details are provided in Appendix B2.

3.3. Net joint power and work

On the paretic limb, peak positive hip power decreased in the P ($p = 0.038$) and BI ($p = 0.014$) conditions relative to UN (Fig. 4A). Peak positive ankle power increased in all powered conditions (P: $p = 0.002$; NP: $p = 0.019$; BI: $p = 0.036$) (Fig. 4C) and positive ankle work increased in all powered conditions (P: $p = 0.003$; NP: $p = 0.021$; BI: $p = 0.005$) (Fig. 5A). On the nonparetic limb, positive hip work increased in the NP ($p < 0.001$) and BI ($p = 0.034$) conditions (Fig. 5A). Positive ankle work also increased in the NP condition ($p = 0.034$) (Fig. 5A). Negative hip work decreased only in the NP condition ($p = 0.002$), but negative knee work decreased in all powered conditions (P: $p < 0.001$; NP: $p = 0.015$; BI: $p < 0.001$) (Fig. 5B).

Overall, positive work of both legs increased in all powered conditions (P: $p = 0.002$; NP: $p < 0.001$; BI: $p = 0.003$) (Fig. 5A). Negative work of both legs decreased only in the P condition ($p = 0.025$) (Fig. 5B). The average peak power and work magnitudes for each joint are provided in Appendix A3 and additional linear mixed effects model details are provided in Appendix B3.

3.4. Joint work distribution

The proportion of paretic hip positive work (i.e., relative to the total positive work of both legs) decreased in the NP condition ($p = 0.005$),

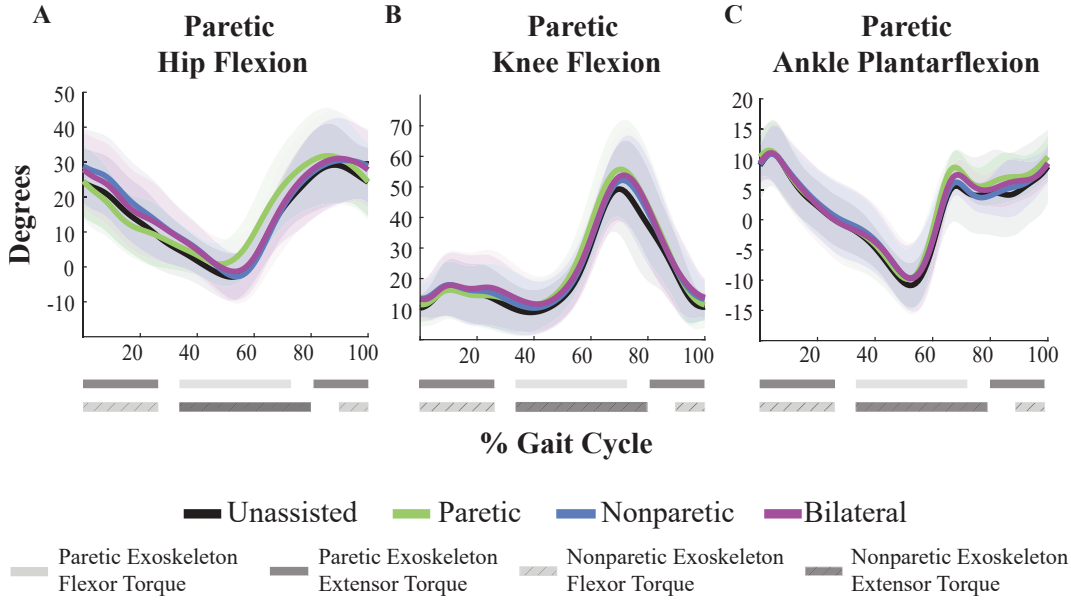

Fig. 2. Average paretic limb (A) hip flexion angle (B) knee flexion angle and (C) ankle plantarflexion angle for all assistance conditions. Shaded regions represent one standard deviation.

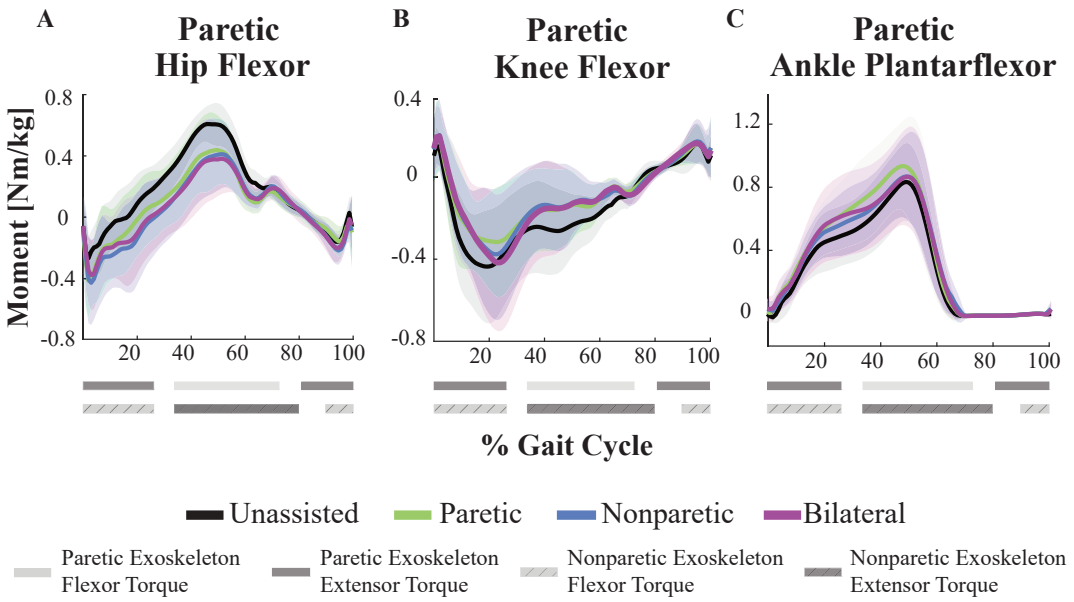

Fig. 3. Average paretic limb net (A) hip flexor moment (B) knee flexor moment and (C) ankle plantarflexor moment. Moments are normalized by body mass and averaged across subjects. Shaded regions represent one standard deviation.

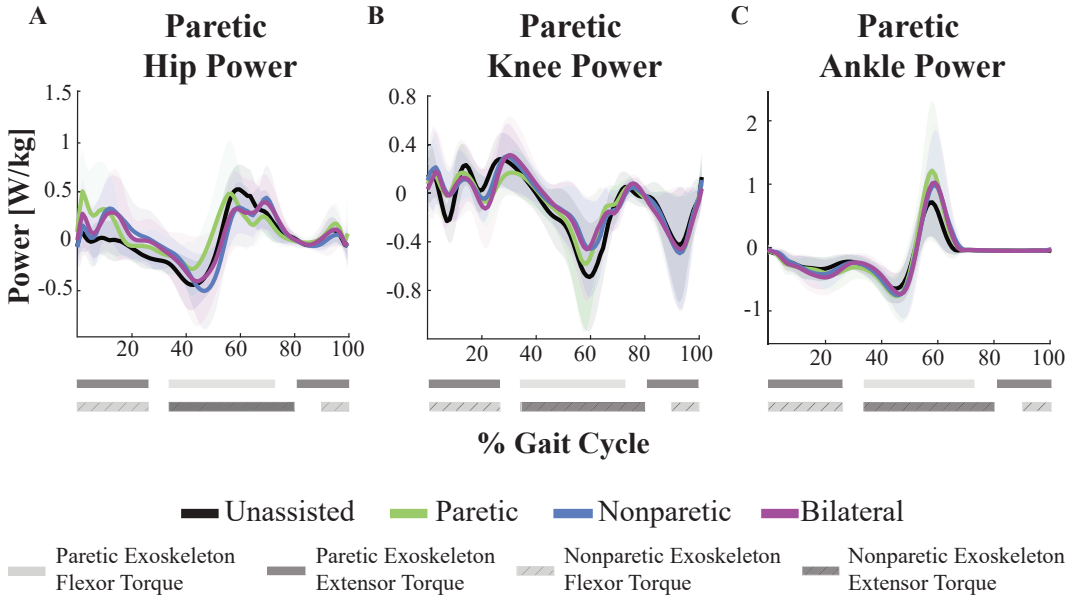

Fig. 4. Average paretic limb net (A) hip power (B) knee power and (C) ankle power. Normalized by body mass and averaged across subjects. Shaded regions represent one standard deviation.

whereas the proportion of nonparetic hip positive work increased in both the NP ($p < 0.001$) and BI ($p = 0.027$) conditions (Fig. 5A). The proportion of paretic knee positive work decreased in the P ($p = 0.005$) and NP ($p = 0.024$) conditions. The proportion of nonparetic ankle positive work decreased only in the BI condition ($p = 0.030$) (Fig. 5A).

The proportion of paretic hip negative work increased only in the NP condition ($p = 0.036$), whereas the proportion of nonparetic hip negative work decreased in the NP condition ($p < 0.001$) (Fig. 5B). The proportion of paretic knee negative work did not change but the proportion of nonparetic knee negative work decreased in the P ($p = 0.005$) and BI ($p < 0.001$) conditions. The proportion of paretic ankle negative work increased in all powered conditions (P: $p < 0.001$; NP: $p < 0.001$; BI: $p = 0.004$) but the proportion of nonparetic ankle negative work increased only in the NP ($p = 0.020$) and BI ($p = 0.017$) conditions (Fig. 5B).

4. Discussion

The purpose of this study was to investigate how different hip exoskeleton limb assistance strategies affect lower-limb joint biomechanics during walking for individuals post-stroke. We first hypothesized that BI assistance would best improve paretic limb late stance leg orientation and swing initiation, which was partially supported as BI assistance did not improve late stance leg orientation but improved peak hip flexion angle and ankle power in late stance. Second, we hypothesized that P assistance would best improve limb asymmetries, which was supported as paretic limb hip and ankle power increased without increasing nonparetic limb joint power. Finally, we hypothesized that NP assistance would indirectly improve P limb late stance leg orientation, which was not supported.

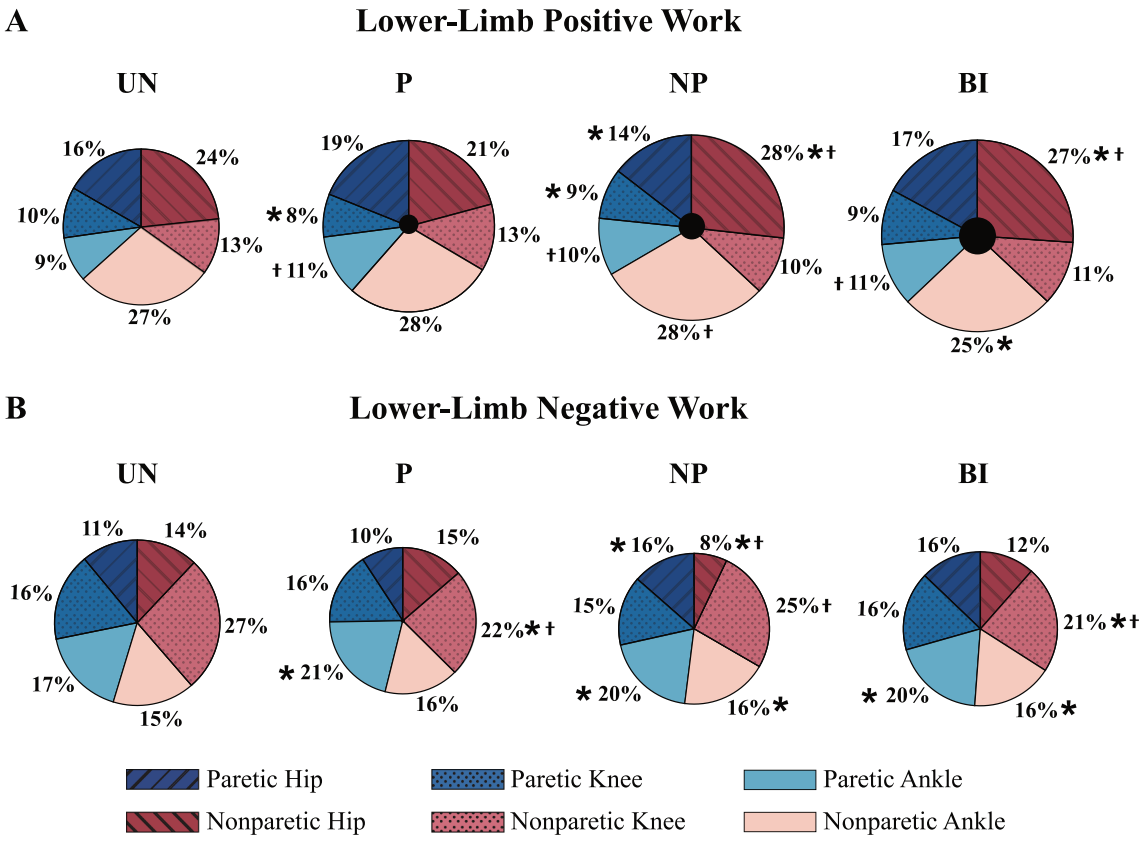

Fig. 5. Joint (A) positive work and (B) negative work distributions across the paretic and nonparetic limbs. Total chart size is normalized by positive and negative magnitude of the strategy relative to UN, respectively. Black center circles represent the exoskeleton work. * represents significant differences in distribution and + represents significant differences in magnitude relative to UN.

4.1. Paretic limb kinematics

Targeted hip joint assistance from the exoskeleton directly altered paretic limb hip kinematics, although flexion and extension assistance did not elicit similar responses. Peak hip flexion angle during swing increased in all powered conditions, suggesting the exoskeleton flexor torque successfully accelerated the leg into swing. However, hip extension angle was only affected in the P condition, which resulted in reduced magnitude and altered timing of peak extension relative to UN. Since the exoskeleton provided hip flexor torque during late stance for swing initiation, the timing of exoskeleton assistance may have decelerated the leg while the hip continued extending in late stance. Since leg extension and step length are typically reduced for individuals post-stroke relative to healthy individuals (Peterson et al., 2010), exoskeleton assistance timing should be carefully tuned to avoid adversely impacting peak hip extension.

Although hip extension was reduced in the P condition, kinematic improvements at the knee were observed, which may be advantageous for individuals exhibiting post-stroke stiff-knee gait. This impairment is characterized by reduced paretic knee flexion in swing (e.g., Akbas et al., 2020; Lee et al., 2024) and may be mitigated by the observed increase in peak knee flexion angle and ROM in the P condition. Stiff-knee gait is also attributed to pre-swing deficits (e.g., Goldberg et al., 2003; Campanini et al., 2013; Bloks et al., 2025), and the exoskeleton flexor torque applied in this phase may help reduce these deficits, highlighting the potential of paretic limb exoskeleton assistance for post-stroke rehabilitation.

4.2. Paretic limb net joint moments

The consistent increase in paretic limb hip extensor moment across all powered conditions suggests that the exoskeleton effectively aided early-stance support. Uniarticular hip extensors, such as the gluteus maximus, are responsible for body support in early stance (e.g., Anderson and Pandy, 2003; Neptune et al., 2004) when the exoskeleton extensor torque is active, which suggests the exoskeleton extensor torque can augment the function of the hip extensors. Individuals post-stroke often have notable asymmetry and rely on their nonparetic limb for support (e.g., Chen et al., 2005; Balasubramanian et al., 2009), thus hip extension assistance may be beneficial for these individuals.

Conversely, net hip flexor moments significantly decreased in all powered conditions. The reduction in hip flexor moment may be partially explained by a reduction in hip flexor muscle output, including the rectus femoris (RF) muscle. Given that the biarticular RF plays a role in both hip flexion and knee extension, the reduction in knee extensor moment observed in the P and NP conditions further suggests reduced RF output. RF has been shown to be hyperactive in individuals post-stroke (e.g., Reinbolt et al., 2008; Tenniglo et al., 2014; Akbas et al., 2019), thereby leading to stiff-knee gait characteristics. Additionally, RF contributes to mid-stance body support for individuals post-stroke (Higginson et al., 2006), so in the case of reduced RF output, the exoskeleton or other muscles, such as the ankle plantarflexors (e.g., Neptune et al., 2001; Anderson and Pandy, 2003), would need to compensate for the reduced support. Peak net ankle plantarflexor moment increased in the P condition, further suggesting the functional role of the plantarflexors may be increased.

Individuals post-stroke also demonstrate merged modular control (Clark et al., 2010), reflecting impaired coordination during gait. Some individuals have exhibited merged muscle modules composed of knee extensors and ankle plantarflexors (Clark et al., 2010), which highlights that impaired coordination between these muscle groups may be linked. Moreover, a reduction in RF and an increase in plantarflexor output

would increase forward propulsion, as RF contributes to braking and the plantarflexors provide forward propulsion (Neptune et al., 2001), which is in agreement with previous studies that observed an increase in peak propulsive forces while wearing a hip exoskeleton (Pan et al., 2023). Healthy individuals have demonstrated reduced RF muscle activity with hip exoskeleton assistance (Lenzi et al., 2013), which aligns with the present reduction in hip flexor moment and highlights a potential response mechanism that can be translated to individuals post-stroke. However, healthy individuals also have reduced ankle plantarflexor activity with hip exoskeleton assistance (Lenzi et al., 2013), unlike the increased ankle plantarflexor moment observed in the present study, which may be more desirable for individuals post-stroke who have reduced plantarflexor output relative to healthy individuals.

4.3. Net joint work

The positive joint work distribution was highly asymmetric in all powered conditions, with most of the joint work done by the nonparetic limb. Previous studies have similarly observed increased nonparetic limb work (Peterson et al., 2011; Farris et al., 2015) and reduced paretic limb energetics (e.g., Chen et al., 2005; Hall et al., 2011) relative to healthy individuals. However, the joint work distribution became more asymmetric in the NP and BI conditions, with greater proportions of nonparetic hip positive work. Previous studies of unassisted walking have shown increased nonparetic hip muscle work for individuals post-stroke, even exceeding the work done by healthy individuals (Peterson et al., 2011). Therefore, further increases in nonparetic hip positive work observed with NP or BI assistance may not be suitable for individuals with elevated nonparetic hip reliance. However, the reduced proportion of nonparetic ankle positive work in the BI condition may help reduce the notable propulsion asymmetries present in individuals post-stroke (Bowden et al., 2006; Roelker et al., 2019). Although the magnitude of paretic ankle positive work increased in all powered conditions, the peak paretic ankle moment only increased in the P condition. A post-hoc analysis of ankle angular velocity revealed that angular velocity increased for all conditions. Thus, increasing ankle power with an exoskeleton is driven predominantly by changes in ankle kinematics rather than ankle moment.

The distribution of negative joint work was more symmetric than positive joint work with roughly half of the negative work done by the paretic limb. The proportion of ankle negative work increased in both limbs in the NP and BI conditions and only the proportion of nonparetic ankle negative work increased in the P condition, which suggests a more distal redistribution of joint work and increased reliance on energy absorption in stance.

Overall, total work across the lower limbs remained unchanged in all powered conditions relative to UN, but there was an increase in positive work for all powered conditions and a reduction in negative work in the P condition. The increase in positive work may reflect the additional work done by the exoskeleton without a notable reduction in overall muscular demand. Future modeling and simulation work is needed to understand how the exoskeleton influences individual muscle output that is reflected in net joint work. However, individuals post-stroke exhibit altered gait patterns that deviate from efficient gait mechanics, suggesting that gait mechanics may improve when walking under less constrained conditions (e.g., walking overground versus at a constant speed on a treadmill). Given that joint power is positively correlated with walking speed (Brincks and Nielsen, 2012; Wonsetler and Bowden, 2017), the observed increase in positive work with exoskeleton assistance suggests that their overground walking speed may increase. This aligns with previous studies showing powered hip exoskeletons can increase overground self-selected walking speed for individuals post-stroke (Pan et al., 2023; Livolsi et al., 2025). Nevertheless, the increase in total positive work was predominantly driven by the nonparetic limb, especially in the NP and BI conditions.

4.4. Limitations & future work

The limited sample size of five participants makes these results difficult to generalize. Individuals post-stroke have high degrees of heterogeneity in their walking mechanics and motor impairments (Appendix C), so future work should use larger sample sizes to improve generalizability. Another limitation is that the exoskeleton controller estimated gait phase kinematics, but individuals post-stroke exhibit asymmetries between limbs. Thus, the commanded torque timing may not have been optimal, and therefore future work should focus on determining the optimal controller for these individuals, as previous work has shown subject-specific controllers can improve performance compared to spline-based controllers (e.g., Zhang et al., 2017; Slade et al., 2024). The individuals were constrained to steady-state walking on the treadmill, so individuals may respond differently to exoskeleton assistance during overground walking. Although constraining the speed in the present study helped reduce variability, isolate joint-level responses and allowed for consistent normalization to 100% of the gait cycle within individuals, it may limit generalizability to real-world walking conditions. The BI condition also utilized an equal assistance magnitude for both limbs. The insights into individual joint responses may help further the development of control schemes for bilateral hip exoskeletons. Further, the experimental net joint measures do not provide insight into what role the exoskeleton and individual muscles play in contributing to biomechanical functions. Rather, the results highlight a response by the individuals wearing the device, so it is unclear if there are additional muscular compensations or interactions to the constrained treadmill environment present to elicit the responses observed. Future work should aim to identify the role of the exoskeleton in improving biomechanical functions to further optimize exoskeleton assistance timing.

5. Conclusion

This study provided insight into the kinematic and kinetic responses of individuals post-stroke walking with different hip exoskeleton limb assistance conditions. These results suggest that paretic limb assistance may improve stiff-knee gait characteristics and promote symmetric joint work between limbs, but bilateral assistance may better help to reduce asymmetrical propulsion. Together, these results highlight the complex biomechanical responses of individuals post-stroke and emphasize the importance of tailoring exoskeleton assistance to improve walking performance.

CRediT authorship contribution statement

Kristen M. Stewart: Writing – original draft, Visualization, Validation, Investigation, Formal analysis, Data curation, Conceptualization. **Gregory S. Sawicki:** Writing – review & editing, Resources, Methodology, Investigation, Data curation, Conceptualization. **Aaron J. Young:** Writing – review & editing, Resources, Methodology, Investigation, Data curation, Conceptualization. **Richard R. Neptune:** Writing – review & editing, Supervision, Resources, Project administration, Methodology, Investigation, Conceptualization.

Declaration of competing interest

The authors declare that they have no known competing financial interests or personal relationships that could have appeared to influence the work reported in this paper.

Acknowledgements

We would like to thank Samsung Electronics for providing the exoskeleton hardware. This work was partially supported by National Institutes of Health Grant No. R03HD097740.

Appendix

Appendix A1. Mean lower-limb joint angles ± one standard deviation. The mean percent increase from the unassisted (UN) condition is denoted in parentheses. Bold indicates a significant difference from the UN condition ($p < 0.05$)

Variable		Unassisted (UN)	Paretic limb (P)	Nonparetic limb (NP)	Bilateral (BI)
Peak Joint Angle (°)					
Hip	Flexion	26.55 ± 8.55	**30.41 ± 10.82 (14.06%)**	**29.82 ± 7.83 (12.51%)**	**31.53 ± 8.28 (22.21%)**
	Extension	7.02 ± 7.62	**3.44 ± 6.07 (−0.94%)**	8.55 ± 6.86 (3.53%)	8.15 ± 9.47 (45.80%)
Knee	Flexion	50.43 ± 11.26	**54.86 ± 14.14 (11.33%)**	51.62 ± 10.36 (3.71%)	52.68 ± 12.91 (5.65%)
	Extension	1.77 ± 9.28	0.98 ± 10.63 (46.03%)	0.12 ± 11.43 (49.22%)	0.94 ± 10.80 (24.15%)
Ankle	Plantarflexion	14.54 ± 6.90	13.64 ± 5.96 (12.08%)	13.39 ± 5.97 (11.58%)	13.46 ± 4.92 (15.00%)
	Dorsiflexion	8.98 ± 3.77	10.12 ± 4.22 (27.33%)	9.54 ± 4.31 (18.41%)	10.08 ± 4.85 (20.34%)
Joint Range of Motion (°)					
Hip		33.58 ± 6.85	33.85 ± 10.56 (2.26%)	**38.38 ± 7.61 (11.12%)**	**39.68 ± 8.28 (18.55%)**
Knee		48.66 ± 13.88	**53.88 ± 16.36 (11.46%)**	52.13 ± 11.24 (6.20%)	50.46 ± 14.73 (7.96%)
Ankle		23.52 ± 4.76	23.76 ± 5.53 (1.74%)	22.70 ± 5.15 (−1.78%)	23.54 ± 5.11 (−1.04%)

Appendix A2. Mean lower-limb net joint moments ± one standard deviation. The mean percent increase from the unassisted (UN) condition is denoted in parentheses. Bold indicates a significant difference from the UN condition ($p < 0.05$)

Variable		Unassisted (UN)	Paretic limb (P)	Nonparetic limb (NP)	Bilateral (BI)
Peak Joint Moment (Nm/kg)					
Hip	Flexor	0.715 ± 0.138	**0.627 ± 0.250 (−16.04%)**	**0.606 ± 0.256 (−21.63%)**	**0.613 ± 0.315 (−15.30%)**
	Extensor	0.295 ± 0.116	**0.426 ± 0.199 (40.40%)**	**0.415 ± 0.199 (37.11%)**	**0.391 ± 0.201 (22.74%)**
Knee	Flexor	0.223 ± 0.114	0.232 ± 0.141 (2.19%)	0.255 ± 0.162 (8.68%)	**0.251 ± 0.146 (12.36%)**
	Extensor	0.484 ± 0.191	0.456 ± 0.193 (2.20%)	0.450 ± 0.194 (−0.12%)	0.483 ± 0.260 (6.16%)
Ankle	Plantarflexor	0.951 ± 0.264	**1.04 ± 0.291 (10.39%)**	1.01 ± 0.268 (2.43%)	0.988 ± 0.313 (3.39%)
	Dorsiflexor	0.041 ± 0.020	0.050 ± 0.029 (23.89%)	**0.034 ± 0.015 (−8.70%)**	0.036 ± 0.028 (−7.48%)
Joint Moment Impulse (Nms/kg)					
Hip	Flexor	0.312 ± 0.100	**0.253 ± 0.120 (–23.52%)**	**0.230 ± 0.118 (−28.11%)**	**0.244 ± 0.137 (–23.16%)**
	Extensor	0.042 ± 0.025	**0.058 ± 0.042 (23.98%)**	**0.070 ± 0.057 (40.80%)**	**0.067 ± 0.051 (43.09%)**
Knee	Flexor	0.066 ± 0.074	0.065 ± 0.069 (−3.32%)	0.074 ± 0.076 (1.82%)	0.068 ± 0.071 (10.08%)
	Extensor	0.210 ± 0.107	**0.167 ± 0.095 (−17.39%)**	**0.150 ± 0.105 (−16.28%)**	0.166 ± 0.116 (−11.04%)
Ankle	Plantarflexor	0.430 ± 0.162	0.450 ± 0.172 (8.55%)	0.431 ± 0.136 (−1.57%)	0.448 ± 0.211 (2.76%)
	Dorsiflexor	0.007 ± 0.003	**0.006 ± 0.002 (−12.44%)**	**0.006 ± 0.001 (−17.95%)**	**0.006 ± 0.002 (−12.56%)**

Appendix A3. Mean lower-limb net joint power ± one standard deviation. The mean percent increase from the unassisted (UN) condition is denoted in parentheses. Bold indicates a significant difference from the UN condition ($p < 0.05$)

Variable		Unassisted (UN)	Paretic limb (P)	Nonparetic limb (NP)	Bilateral (BI)
Peak Joint Power (W/kg)					
Hip	Positive	0.595 ± 0.263	0.843 ± 0.644 (38.35%)	0.630 ± 0.293 (−4.47%)	0.762 ± 0.495 (36.12%)
	Negative	−0.611 ± 0.197	−0.603 ± 0.256 (17.01%)	−0.784 ± 0.410 (21.87%)	−0.758 ± 0.491 (33.54%)
Knee	Positive	0.462 ± 0.141	0.505 ± 0.165 (20.30%)	0.497 ± 0.147 (18.16%)	0.544 ± 0.187 (29.13%)
	Negative	−0.756 ± 0.324	−0.715 ± 0.468 (−9.21%)	−0.649 ± 0.364 (−16.68%)	−0.682 ± 0.371 (2.35%)
Ankle	Positive	0.791 ± 0.441	**1.22 ± 0.907 (44.10%)**	**1.02 ± 0.695 (17.66%)**	**1.04 ± 0.741 (28.18%)**
	Negative	−0.728 ± 0.304	−0.806 ± 0.324 (11.54%)	−0.791 ± 0.325 (7.95%)	−0.805 ± 0.341 (5.91%)
Joint Work (J/kg)					
Hip	Positive	0.129 ± 0.053	0.177 ± 0.132 (36.70%)	0.142 ± 0.089 (−6.56%)	0.155 ± 0.104 (30.38%)
	Negative	−0.134 ± 0.049	−0.103 ± 0.075 (−27.66%)	−0.162 ± 0.111 (9.98%)	−0.168 ± 0.149 (12.65%)
Knee	Positive	0.084 ± 0.024	0.077 ± 0.021 (2.16%)	0.085 ± 0.023 (5.72%)	0.088 ± 0.032 (12.36%)
	Negative	−0.187 ± 0.073	−0.174 ± 0.092 (−10.98%)	−0.149 ± 0.077 (−18.35%)	−0.167 ± 0.089 (−0.55%)
Ankle	Positive	0.078 ± 0.042	**0.110 ± 0.077 (30.04%)**	**0.100 ± 0.062 (18.95%)**	**0.106 ± 0.072 (29.06%)**
	Negative	−0.206 ± 0.069	−0.217 ± 0.072 (11.56%)	−0.202 ± 0.061 (1.01%)	−0.210 ± 0.072 (3.90%)

Appendix B1. Linear mixed effects model details for joint angle measures

Measure		Linear mixed effects model p-value	Random effects			Condition	Beta coefficients 95% CI		Follow-up *t*-test p-value
			Standard deviation	95% CI Lower	Upper		Lower	Upper	
Hip Angle	Peak Flexion	**<0.001**	7.96	4.26	14.85	UN	19.56	33.88	
						P	2.05	5.42	**0.004**
						NP	1.24	4.53	**<0.001**
						BI	2.98	6.31	**<0.001**
	Peak Extension	**<0.001**	6.58	3.52	12.30	UN	1.32	13.19	
						P	−4.52	−1.61	**0.002**
						NP	−0.59	2.32	1.00
						BI	−0.81	2.21	1.00
	ROM	**0.003**	6.65	3.53	12.54	UN	27.81	40.14	
						P	−1.28	3.74	1.00
						NP	1.26	6.23	**0.003**
						BI	2.86	8.07	**0.001**
Knee Angle	Peak Flexion	**<0.001**	11.20	6.00	20.88	UN	40.60	60.72	
						P	2.71	6.88	**0.002**
						NP	−0.61	3.57	0.197
						BI	1.86	6.40	0.620
	Peak Extension	0.262	9.88	5.30	18.39	UN	−7.58	10.06	
						P	−1.45	1.26	
						NP	−2.28	0.43	
						BI	−2.48	0.23	
	ROM	**<0.001**	13.39	7.17	24.98	UN	37.13	61.21	
						P	2.85	8.31	**<0.001**
						NP	−0.31	5.14	0.247
						BI	1.05	6.51	0.100
Ankle Angle	Peak Plantarflexion	0.365	5.21	2.79	9.73	UN	10.94	20.37	
						P	−3.34	−0.80	
						NP	−3.30	−0.85	
						BI	−3.32	−0.87	
	Peak Dorsiflexion	0.077	4.14	2.22	7.74	UN	4.30	11.79	
						P	1.00	3.37	
						NP	0.40	2.59	
						BI	0.72	2.69	
	ROM	0.543	4.74	2.54	8.85	UN	19.42	27.97	
						P	−0.74	1.29	
						NP	−1.49	0.55	
						BI	−1.41	0.63	

Appendix B2. Linear mixed effects model details for joint moment measures

Measure		Linear mixed effects model p-value	Random effects			Condition	Beta coefficients 95% CI		Follow-up *t*-test p-value
			Standard deviation	95% CI Lower	Upper		Lower	Upper	
Hip Moment	Peak Flexor	**<0.001**	0.216	0.115	0.404	UN	0.527	0.918	
						P	0.002	−0.139	**0.041**
						NP	0.000	−0.185	**0.008**
						BI	0.000	−0.156	**0.017**
	Peak Extensor	**<0.001**	0.174	0.093	0.324	UN	0.132	0.445	
						P	0.091	0.161	**<0.001**
						NP	0.095	0.164	**<0.001**
						BI	0.050	0.120	**0.003**
	Flexor Impulse	**<0.001**	0.106	0.056	0.198	UN	0.225	0.417	
						P	−0.096	−0.040	**<0.001**
						NP	−0.116	−0.060	**0.001**
						BI	−0.099	−0.043	**0.001**
	Extensor Impulse	**<0.001**	0.038	0.020	0.071	UN	0.009	0.077	
						P	0.006	0.020	**0.010**
						NP	0.011	0.032	**0.006**
						BI	0.015	0.029	**0.002**
Knee Moment	Peak Flexor	**0.025**	0.136	0.073	0.253	UN	0.103	0.346	
						P	−0.012	0.036	1.00
						NP	0.003	0.051	0.260
						BI	0.007	0.055	**0.026**
	Peak Extensor	0.674	0.182	0.097	0.341	UN	0.308	0.640	
						P	−0.047	0.065	
						NP	−0.062	0.050	
						BI	−0.038	0.074	
	Flexor Impulse	**0.011**	0.074	0.040	0.137	UN	0.002	0.133	
						P	−0.006	0.001	1.00
						NP	−0.001	0.006	0.608
						BI	0.001	0.007	0.287
	Extensor Impulse	**0.002**	0.088	0.047	0.164	UN	0.136	0.296	
						P	−0.075	−0.022	**0.016**
						NP	−0.083	−0.030	**0.050**
						BI	−0.070	−0.018	0.218
Ankle Moment	Peak Plantarflexor	**<0.001**	0.273	0.147	0.508	UN	0.714	1.200	
						P	0.050	0.115	**<0.001**
						NP	−0.006	0.058	0.855
						BI	0.016	0.080	0.938
	Peak Dorsiflexor	**<0.001**	0.018	0.010	0.035	UN	0.026	0.059	
						P	−0.003	0.010	1.00
						NP	−0.015	−0.003	**0.040**
						BI	−0.013	−0.001	0.531
	Plantarflexor Impulse	**0.016**	0.157	0.084	0.292	UN	0.284	0.564	
						P	0.002	0.050	0.114
						NP	−0.033	0.014	0.617
						BI	−0.010	0.037	0.868
	Dorsiflexor Impulse	**<0.001**	0.001	0.001	0.003	UN	0.005	0.008	
						P	−0.001	0.000	**0.010**
						NP	−0.002	−0.001	**0.002**
						BI	−0.001	−0.000	**0.033**

Appendix B3. Linear mixed effects model details for joint power measures

Measure		Linear mixed effects model p-value	Random effects			Condition	Beta coefficients 95% CI		Follow-up *t*-test p-value
			Standard deviation	95% CI Lower	Upper		Lower	Upper	
Hip Power	Peak Positive	**<0.001**	0.322	0.171	0.606	UN	0.297	0.889	
						P	0.042	0.263	**0.038**
						NP	−0.129	0.084	1.00
						BI	0.077	0.296	**0.014**
	Peak Negative	0.150	0.233	0.122	0.446	UN	−0.797	−0.346	
						P	−0.180	0.074	
						NP	−0.319	−0.067	
						BI	−0.262	−0.004	
	Positive Work	**0.002**	0.076	0.041	0.144	UN	0.062	0.203	
						P	0.024	0.081	0.053
						NP	−0.026	0.029	1.00
						BI	0.004	0.060	0.127
	Negative Work	**0.005**	0.078	0.041	0.146	UN	−0.207	−0.064	
						P	−0.001	0.051	0.093
						NP	−0.057	−0.004	0.469
						BI	−0.044	0.009	1.00
Knee Power	Peak Positive	0.068	0.089	0.045	0.176	UN	0.357	0.543	
						P	−0.007	0.137	
						NP	0.016	0.157	
						BI	0.049	0.191	
	Peak Negative	0.082	0.329	0.175	0.617	UN	−1.044	−0.443	
						P	−0.060	0.137	
						NP	0.011	0.209	
						BI	−0.093	0.107	
	Positive Work	0.538	0.019	0.010	0.036	UN	0.064	0.100	
						P	−0.010	0.012	
						NP	−0.007	0.014	
						BI	−0.003	0.018	
	Negative Work	**0.033**	0.073	0.039	0.137	UN	−0.264	−0.131	
						P	0.010	0.048	0.536
						NP	0.024	0.063	0.051
						BI	0.008	0.048	1.00
Ankle Power	Peak Positive	**<0.001**	0.665	0.357	1.24	UN	0.262	1.451	
						P	0.186	0.384	**0.002**
						NP	0.041	0.238	**0.019**
						BI	0.066	0.263	**0.036**
	Peak Negative	0.131	0.290	0.155	0.542	UN	−0.981	−0.456	
						P	−0.151	−0.001	
						NP	−0.143	0.006	
						BI	−0.108	0.041	
	Positive Work	**<0.001**	0.061	0.033	0.115	UN	0.030	0.140	
						P	0.013	0.029	**0.003**
						NP	0.005	0.021	**0.021**
						BI	0.012	0.028	**0.005**
	Negative Work	**0.011**	0.067	0.036	0.126	UN	−0.265	−0.144	
						P	−0.030	−0.003	0.202
						NP	−0.010	0.017	1.00
						BI	−0.019	0.008	0.813

Appendix C1. Individual subject average hip flexion angles for all conditions

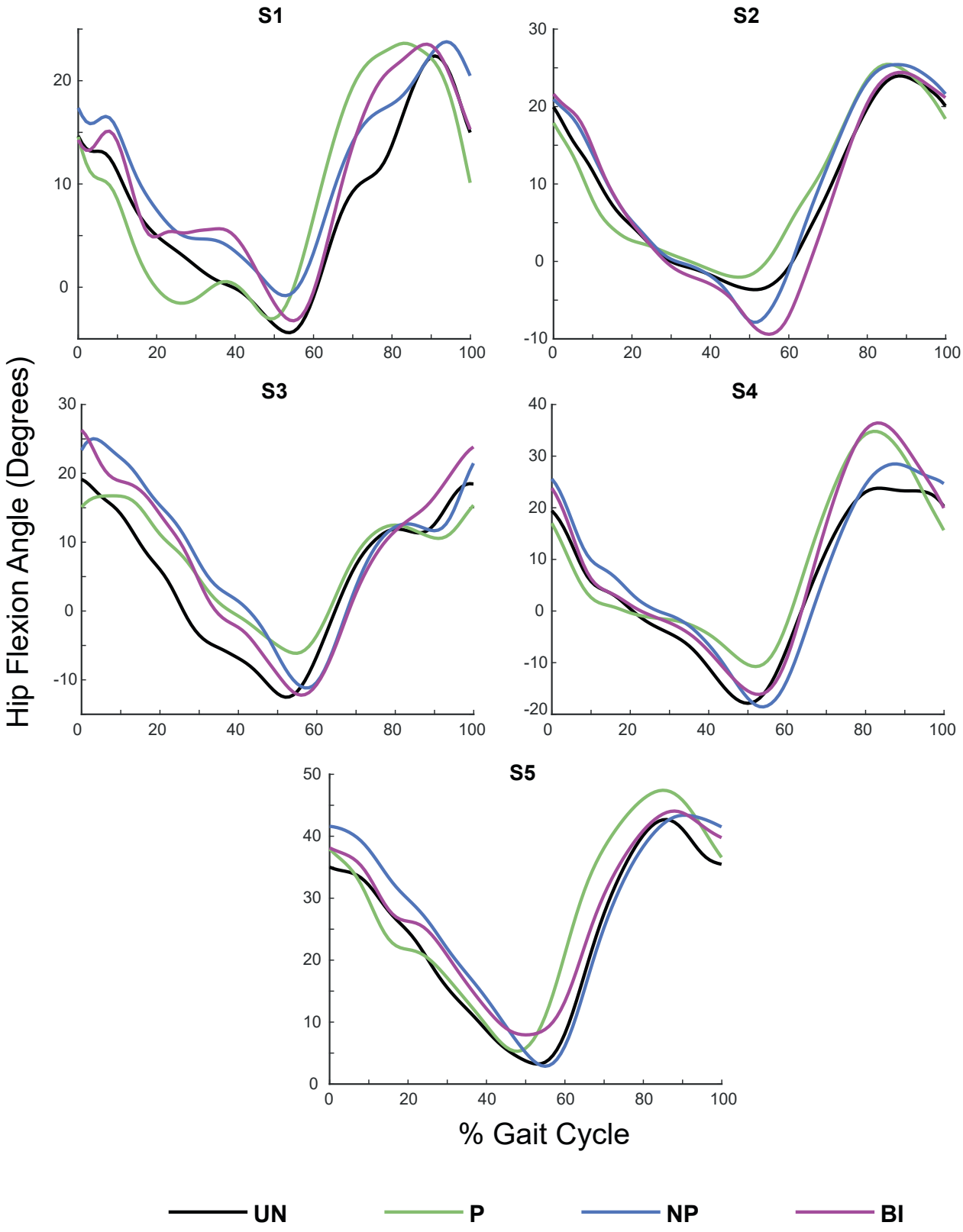

Appendix C2. Individual subject average hip flexor moments for all conditions

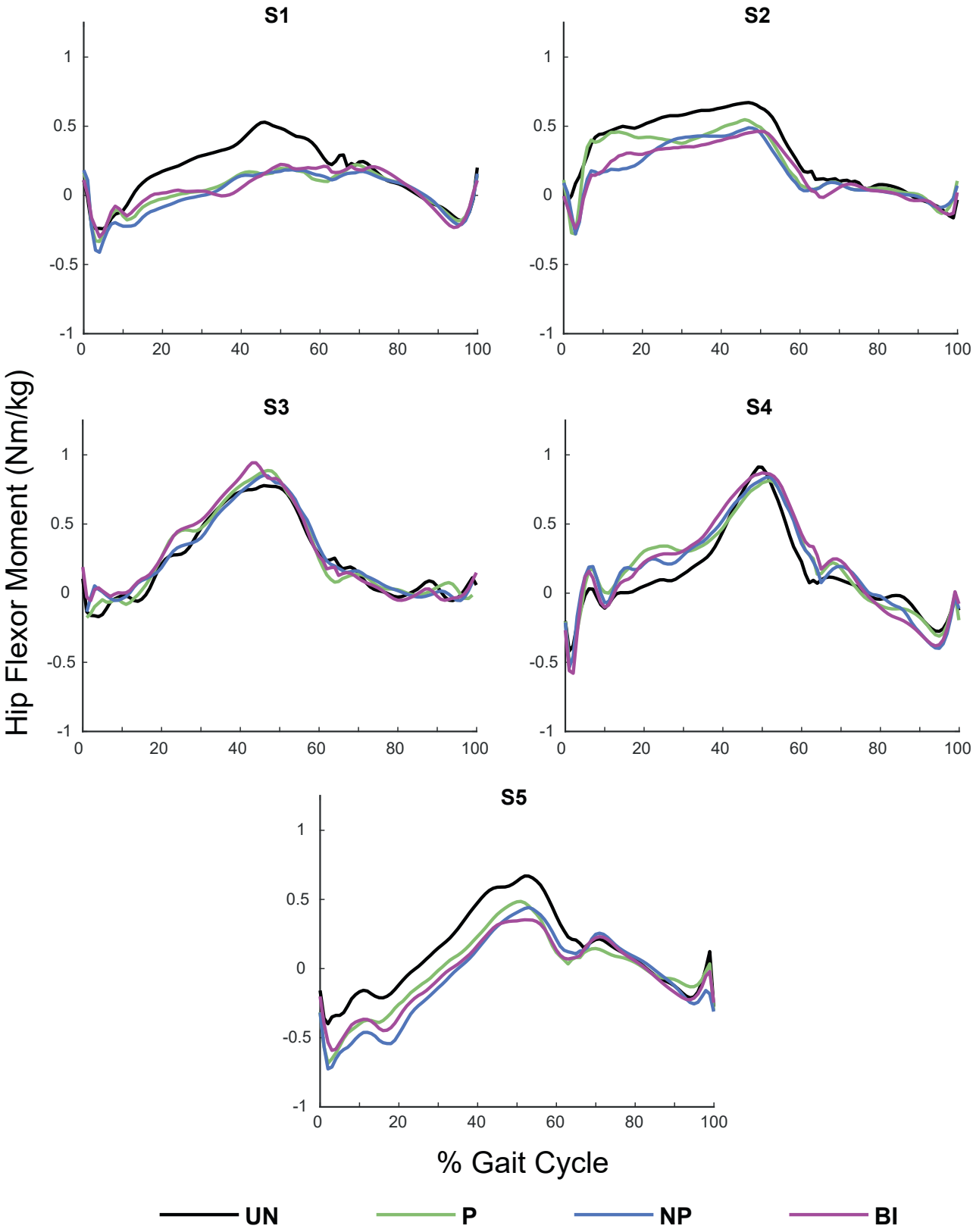

Appendix C3. Individual subject average hip power for all conditions

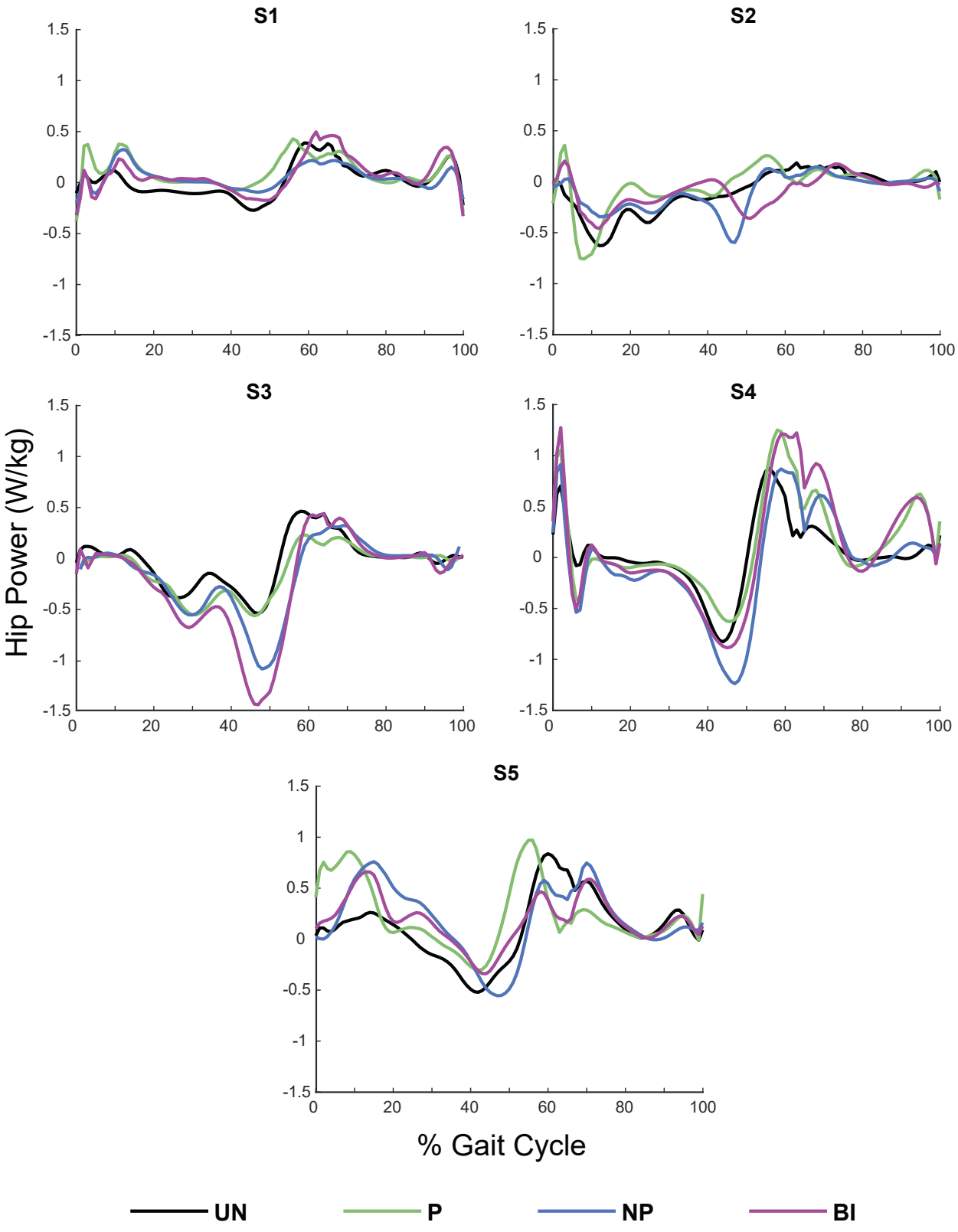

References

Akbas, T., Kim, K., Doyle, K., Manella, K., Lee, R., Spicer, P., Knikou, M., Sulzer, J., 2020. Rectus femoris hyperreflexia contributes to Stiff-knee gait after stroke. J. Neuroeng. Rehabil. 17 (1), 117. https://doi.org/10.1186/s12984-020-00724-z.

Akbas, T., Neptune, R.R., Sulzer, J., 2019. Neuromusculoskeletal simulation reveals Abnormal Rectus Femoris-Gluteus Medius Coupling in Post-stroke Gait. Front. Neurol. 10. https://doi.org/10.3389/fneur.2019.00301.

Anderson, F.C., Pandy, M.G., 2003. Individual muscle contributions to support in normal walking. Gait Posture 17 (2), 159–169. https://doi.org/10.1016/S0966-6362(02)00073-5.

Awad, L.N., Bae, J., O'donnell, K., De Rossi, S.M., Hendron, K., Sloot, L.H., Kudzia, P., Allen, S., Holt, K.G., Ellis, T.D., Walsh, C.J., 2017. A soft robotic exosuit improves walking in patients after stroke. Science translational medicine 9 (400), eaai9084. https://doi.org/10.1126/scitranslmed.aai9084.

Balasubramanian, C.K., Neptune, R.R., Kautz, S.A., 2009. Variability in spatiotemporal step characteristics and its relationship to walking performance post-stroke. Gait Posture 29 (3), 408–414. https://doi.org/10.1016/j.gaitpost.2008.10.061.

Bloks, B.E., Keijsers, N.L., van Oorschot, W., Geurts, A.C., Nonnekes, J., 2025. Towards a precision rehabilitation approach for post-stroke stiff knee gait. Clin. Biomech., 106587 https://doi.org/10.1016/j.clinbiomech.2025.106587.

Bowden, M.G., Balasubramanian, C.K., Neptune, R.R., Kautz, S.A., 2006. Anterior-Posterior Ground Reaction Forces as a measure of Paretic Leg Contribution in Hemiparetic walking. Stroke 37 (3), 872–876. https://doi.org/10.1161/01.STR.0000204063.75779.8d.

Brandstater, M.E., de Bruin, H., Gowland, C., Clark, B.M., 1983. Hemiplegic gait: Analysis of temporal variables. Arch. Phys. Med. Rehabil. 64 (12), 583–587.

Brincks, J., Nielsen, J.F., 2012. Increased power generation in impaired lower extremities correlated with changes in walking speeds in sub-acute stroke patients. Clin. Biomech. 27 (2), 138–144. https://doi.org/10.1016/j.clinbiomech.2011.08.007.

Bryan, G.M., Franks, P.W., Song, S., Voloshina, A.S., Reyes, R., O'Donovan, M.P., Gregorczyk, K.N., Collins, S.H., 2021. Optimized hip–knee–ankle exoskeleton assistance at a range of walking speeds. J. Neuroeng. Rehabil. 18 (1), 152. https://doi.org/10.1186/s12984-021-00943-y.

Campanini, I., Merlo, A., Damiano, B., 2013. A method to differentiate the causes of stiff-knee gait in stroke patients. Gait Posture 38 (2), 165–169. https://doi.org/10.1016/j.gaitpost.2013.05.003.

Chen, G., Patten, C., Kothari, D.H., Zajac, F.E., 2005. Gait differences between individuals with post-stroke hemiparesis and non-disabled controls at matched speeds. Gait Posture 22 (1), 51–56. https://doi.org/10.1016/j.gaitpost.2004.06.009.

Clark, D.J., Ting, L.H., Zajac, F.E., Neptune, R.R., Kautz, S.A., 2010. Merging of healthy Motor Modules Predicts Reduced Locomotor Performance and Muscle Coordination Complexity Post-Stroke. J. Neurophysiol. 103 (2), 844–857. https://doi.org/10.1152/jn.00825.2009.

Dean, J.C., Bowden, M.G., Kelly, A.L., Kautz, S.A., 2020. Altered post-stroke propulsion is related to paretic swing phase kinematics. Clin. Biomech. 72, 24–30. https://doi.org/10.1016/j.clinbiomech.2019.11.024.

Ding, Y., Kim, M., Kuindersma, S., Walsh, C.J., 2018. Human-in-the-loop optimization of hip assistance with a soft exosuit during walking. Sci. Rob. 3 (15), eaar5438. https://doi.org/10.1126/scirobotics.aar5438.

Farris, D.J., Hampton, A., Lewek, M.D., Sawicki, G.S., 2015. Revisiting the mechanics and energetics of walking in individuals with chronic hemiparesis following stroke: from individual limbs to lower limb joints. J. Neuroeng. Rehabil. 12 (1), 24. https://doi.org/10.1186/s12984-015-0012-x.

Galle, S., Malcolm, P., Collins, S.H., De Clercq, D., 2017. Reducing the metabolic cost of walking with an ankle exoskeleton: Interaction between actuation timing and power. J. Neuroeng. Rehabil. 14 (1), 35. https://doi.org/10.1186/s12984-017-0235-0.

Goldberg, S.R., Õunpuu, S., Delp, S.L., 2003. The importance of swing-phase initial conditions in stiff-knee gait. J. Biomech. 36 (8), 1111–1116. https://doi.org/10.1016/S0021-9290(03)00106-4.

Hall, A.L., Peterson, C.L., Kautz, S.A., Neptune, R.R., 2011. Relationships between muscle contributions to walking subtasks and functional walking status in persons with post-stroke hemiparesis. Clin. Biomech. 26 (5), 509–515. https://doi.org/10.1016/j.clinbiomech.2010.12.010.

Higginson, J.S., Zajac, F.E., Neptune, R.R., Kautz, S.A., Delp, S.L., 2006. Muscle contributions to support during gait in an individual with post-stroke hemiparesis. J. Biomech. 39 (10), 1769–1777. https://doi.org/10.1016/j.jbiomech.2005.05.032.

Kang, I., Molinaro, D.D., Duggal, S., Chen, Y., Kunapuli, P., Young, A.J., 2021. Real-Time Gait phase Estimation for Robotic Hip Exoskeleton Control during Multimodal Locomotion. IEEE Rob. Autom. Lett. 6 (2), 3491–3497. https://doi.org/10.1109/LRA.2021.3062562.

Langhorne, P., Bernhardt, J., Kwakkel, G., 2011. Stroke rehabilitation. Lancet 377 (9778), 1693–1702. https://doi.org/10.1016/S0140-6736(11)60325-5.

Lee, H.-J., Lee, S.-H., Seo, K., Lee, M., Chang, W.H., Choi, B.-O., Ryu, G.-H., Kim, Y.-H., 2019. Training for walking Efficiency with a Wearable Hip-Assist Robot in patients with Stroke. Stroke 50 (12), 3545–3552. https://doi.org/10.1161/STROKEAHA.119.025950.

Lee, J., Lee, R.K., Seamon, B.A., Kautz, S.A., Neptune, R.R., Sulzer, J., 2024. Between-limb difference in peak knee flexion angle can identify persons post-stroke with Stiff-knee gait. Clin. Biomech. 120, 106351. https://doi.org/10.1016/j.clinbiomech.2024.106351.

Lenzi, T., Carrozza, M.C., Agrawal, S.K., 2013. Powered Hip Exoskeletons can Reduce the User's Hip and Ankle Muscle Activations during walking. IEEE Trans. Neural Syst. Rehabil. Eng. 21 (6), 938–948. https://doi.org/10.1109/TNSRE.2013.2248749.

Livolsi, C., Conti, R., Ciapetti, T., Guanziroli, E., Fridriksson, T., Alexandersson, Á., Trigili, E., Giovacchini, F., Lova, R.M., Esquenazi, A., Molteni, F., Crea, S., Vitiello, N., 2025. Bilateral hip exoskeleton assistance enables faster walking in individuals with chronic stroke-related gait impairments. Sci. Rep. 15 (1), 2017. https://doi.org/10.1038/s41598-025-86343-x.

Mahon, C.E., Farris, D.J., Sawicki, G.S., Lewek, M.D., 2015. Individual limb mechanical analysis of gait following stroke. J. Biomech. 48 (6), 984–989. https://doi.org/10.1016/j.jbiomech.2015.02.006.

McCain, E.M., Dick, T.J.M., Giest, T.N., Nuckols, R.W., Lewek, M.D., Saul, K.R., Sawicki, G.S., 2019. Mechanics and energetics of post-stroke walking aided by a powered ankle exoskeleton with speed-adaptive myoelectric control. J. Neuroeng. Rehabil. 16 (1), 57. https://doi.org/10.1186/s12984-019-0523-y.

Neptune, R.R., Kautz, S.A., Zajac, F.E., 2001. Contributions of the individual ankle plantar flexors to support, forward progression and swing initiation during walking. J. Biomech. 34 (11), 1387–1398. https://doi.org/10.1016/S0021-9290(01)00105-1.

Neptune, R.R., Zajac, F.E., Kautz, S.A., 2004. Muscle force redistributes segmental power for body progression during walking. Gait Posture 19 (2), 194–205. https://doi.org/10.1016/S0966-6362(03)00062-6.

Olney, S.J., Richards, C., 1996. Hemiparetic gait following stroke. Part I: Characteristics. Gait Posture 4 (2), 136–148. https://doi.org/10.1016/0966-6362(96)01063-6.

Pan, Y.-T., Kang, I., Joh, J., Kim, P., Herrin, K.R., Kesar, T.M., Sawicki, G.S., Young, A.J., 2023. Effects of Bilateral Assistance for Hemiparetic Gait Post-Stroke using a Powered Hip Exoskeleton. Ann. Biomed. Eng. 51 (2), 410–421. https://doi.org/10.1007/s10439-022-03041-9.

Peterson, C.L., Cheng, J., Kautz, S.A., Neptune, R.R., 2010. Leg extension is an important predictor of paretic leg propulsion in hemiparetic walking. Gait Posture 32 (4), 451–456. https://doi.org/10.1016/j.gaitpost.2010.06.014.

Peterson, C.L., Kautz, S.A., Neptune, R.R., 2011. Muscle work is increased in pre-swing during hemiparetic walking. Clin. Biomech. 26 (8), 859–866. https://doi.org/10.1016/j.clinbiomech.2011.04.010.

Reinbolt, J.A., Fox, M.D., Arnold, A.S., Õunpuu, S., Delp, S.L., 2008. Importance of preswing rectus femoris activity in stiff-knee gait. J. Biomech. 41 (11), 2362–2369. https://doi.org/10.1016/j.jbiomech.2008.05.030.

Roelker, S.A., Bowden, M.G., Kautz, S.A., Neptune, R.R., 2019. Paretic propulsion as a measure of walking performance and functional motor recovery post-stroke: a review. Gait Posture 68, 6–14. https://doi.org/10.1016/j.gaitpost.2018.10.027.

Seo, K., Lee, J., Lee, Y., Ha, T., Shim, Y., 2016. Fully autonomous hip exoskeleton saves metabolic cost of walking. In: 2016 IEEE International Conference on Robotics and Automation (ICRA), pp. 4628–4635. https://doi.org/10.1109/ICRA.2016.7487663.

Slade, P., Atkeson, C., Donelan, J.M., Houdijk, H., Ingraham, K.A., Kim, M., Kong, K., Poggensee, K.L., Riener, R., Steinert, M., Zhang, J., Collins, S.H., 2024. On human-in-the-loop optimization of human–robot interaction. Nature 633 (8031), 779–788. https://doi.org/10.1038/s41586-024-07697-2.

Tenniglo, M.J., Nederhand, M.J., Prinsen, E.C., Nene, A.V., Rietman, J.S., Buurke, J.H., 2014. Effect of Chemodenervation of the Rectus Femoris Muscle in adults with a Stiff knee Gait due to Spastic Paresis: a Systematic Review with a Meta-Analysis in patients with Stroke. Arch. Phys. Med. Rehabil. 95 (3), 576–587. https://doi.org/10.1016/j.apmr.2013.11.008.

Wonsetler, E.C., Bowden, M.G., 2017. A systematic review of mechanisms of gait speed change post-stroke. Part 1: Spatiotemporal parameters and asymmetry ratios. Top. Stroke Rehabil. 24 (6), 435–446. https://doi.org/10.1080/10749357.2017.1285746.

Young, A.J., Foss, J., Gannon, H., Ferris, D.P., 2017. Influence of Power delivery timing on the Energetics and Biomechanics of Humans Wearing a Hip Exoskeleton. Front. Bioeng. Biotechnol. 5. https://doi.org/10.3389/fbioe.2017.00004.

Zhang, J., Fiers, P., Witte, K.A., Jackson, R.W., Poggensee, K.L., Atkeson, C.G., Collins, S.H., 2017. Human-in-the-loop optimization of exoskeleton assistance during walking. Science 356 (6344), 1280–1284. https://doi.org/10.1126/science.aal5054.